Structure and Phase Transitions of Molybdenum(III) Sulfide and Some Related Phases†

R. DE JONGE, T. J. A. POPMA, G. A. WIEGERS, AND F. JELLINEK

Laboratorium voor Anorganische Chemie, Rijksuniversiteit, Groningen, The Netherlands

Molybdenum(III) sulfide, $Mo_{2.06}S_3$, is monoclinic with $a = 6.092$ Å; $b = 3.208$ Å; $c = 8.6335$ Å; $\beta = 102.43°$. The structure has been determined and refined from X-ray powder data. The metal atoms lie in octahedral holes of a *chh* close packing of sulfur, but they are displaced from the octahedron centers in such a way that zigzag Mo–Mo chains are formed (Mo–Mo = 2.86 Å). Below +37°C the structure is a superstructure of the one described, all axes being doubled. At −80°C the lattice of $Mo_{2.06}S_3$ undergoes a distortion to triclinic symmetry. In solid solutions $(Mo_{1-x}, Nb_x)_{2.06}S_3$ with $0.025 < x \leqslant 0.50$ no superstructures are observed; the structure remains monoclinic down to low temperatures. The compounds previously regarded as Mo_2Se_3 and Mo_2Te_3 are better designated as Mo_3Se_4 and Mo_3Te_4. The low-temperature Guinier camera used in this investigation is described.

Introduction

The outlines of the crystal structure of molybdenum(III) sulfide have been reported by one of the present authors (*1*). The compound was described as monoclinic with $a = 6.092$ Å; $b = 3.208$ Å; $c = 8.633^5$ Å; $\beta = 102.43°$ at room temperature; the space group was given as $P2_1/m - C_{2h}^2$ with all atoms in position $2(e): \pm(x\frac{1}{4}z)$.

In the present study a refinement of the structure is reported. It was found, however, that this structure is only a substructure of the true one; at room temperature all axes should be doubled. The doubling of the axes disappears at +37°C. By means of a low-temperature Guinier camera a further transition was found at −80°C; at lower temperature the symmetry of the lattice is triclinic.

The phase molybdenum(III) sulfide has a narrow range of homogeneity. Chemical analysis showed the composition to be $Mo_{2.06}S_3$, in agreement with other investigators (*2, 3*). Up to half of the Mo atoms can be replaced by Nb; in the solid solutions $(Mo_{1-x}, Nb_x)_{2.06}S_3$ the high-temperature structure of $Mo_{2.06}S_3$ is retained down to low temperatures if $0.025 < x \leqslant 0.50$.

The phases previously regarded as "Mo_2Se_3" and "Mo_2Te_3" were found to contain even larger proportions of metal than $Mo_{2.06}S_3$. Since the composition Mo_3X_4 lies within the broad homogeneity ranges of these phases (while composition Mo_2X_3 does not), the phases are better described as Mo_3Se_4 and Mo_3Te_4, respectively.

Experimental

Molybdenum(III) sulfide was prepared by heating mixtures of the elements in evacuated quartz tubes at 1300°C for sixty hours and quenching to room temperature; the reaction tube was enclosed in another quartz tube filled with argon. Pure well-crystallized samples were obtained if the starting atomic ratio Mo:S was 2.06:3; in some cases needle-shaped crystals up to 10 mm in length were obtained. For deviating atomic ratios Mo or MoS_2 were found as contaminants. Contamination of the product by MoS_2 was also observed if the heating temperature was 1100°C or lower. Solid solutions $(Mo_{1-x}, Nb_x)_{2.06}S_3$ were prepared in the same way as $Mo_{2.06}S_3$; for $x > 0.50$ inhomogeneous products were obtained. Mo_3Se_4 was prepared in the same way as the sulfide; Mo_3Te_4 was prepared from the elements at 900°C.

Differential thermal analyses were carried out with apparatus constructed by Drs. J. C. Wildervanck and J. Koopstra.
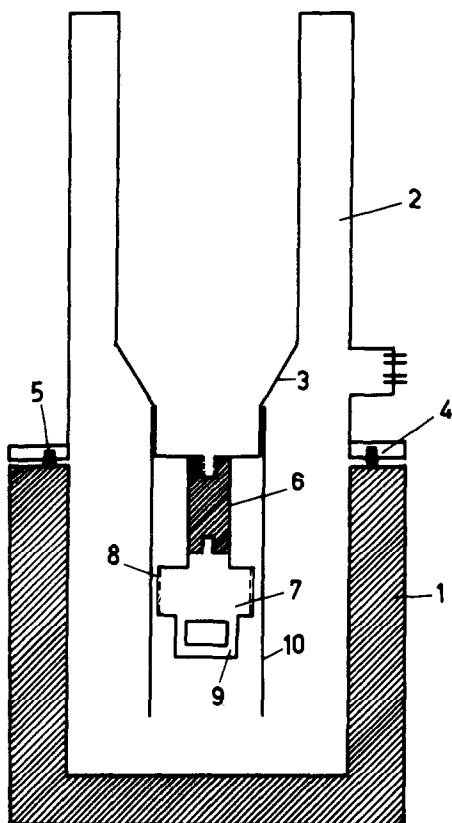
FIG. 1. Low-temperature attachment of the Guinier–Lenné camera (not on scale); for explanation see text.

X-ray diagrams of single crystals were taken with a Weissenberg camera (Nonius), powder diagrams at room temperature with a diffractometer (Philips) and a Guinier–De Wolff camera (Nonius), powder diagrams at higher temperatures with a Guinier–Lenné camera (4) (Nonius); CuK_α radiation was used in all cases.

Low-Temperature Guinier Camera

X-ray powder diagrams at temperatures between $+20$ and $-180°C$ were taken by means of a Guinier–Lenné camera (Nonius) adapted for working at low temperatures. The camera top of the Guinier–Lenné high-temperature camera (4) with sample holder and furnace was replaced by a cold-finger cryostat. A general view is given in Fig. 1.

The dewar (2) consists of two concentric nickel-silver cylinders; the inner cylinder which has a copper base (3), is suspended from the top. The outer cylinder has a brass flange (4) which can be bolted to the vacuum chamber (1); the connection is sealed by an O-ring (5).

The sample holder (7) is made of copper; it is

connected to the base of the dewar by a stainless-steel bar (6). The upper part of the sample holder is enveloped by a heating coil (8) of 0.3-mm insulated nichrome wire; the lower part is identical to the sample holder of the high-temperature camera. The powdered sample is pressed on a silver gauze (250 mesh) of dimensions $15 \times 7 \times 0.06$ mm; the gauze supported by two silver windows is placed in the sample holder. The copper radiation shield (10) is cooled by contact with the dewar base. The shield has a window of 8×8 mm for the primary X-ray beam and a window of 100 circular degrees with a height of 8 mm for the diffracted radiation.

The temperature of the sample is measured with a copper–constantan thermocouple (9). To avoid heat leaks the leads to the thermocouple and the heating coil are spiraled and taken out through a glass–metal seal in the outer cylinder of the dewar. The sample temperature is varied continuously by regulating the power in the heating coil by means of the same temperature-programming unit as used for the high-temperature camera. (About 30 W was needed to obtain room temperature when liquid nitrogen was used as the cooling liquid.) During the exposures the level of the cooling liquid is kept constant by connecting the dewar with a large container using a level-sensitive device with a thermistor; for safety, a second thermistor is situated near the bottom of the dewar.

Substructure of $Mo_{2.06}S_3$

It was attempted to refine the structure of $Mo_{2.06}S_3$ from X-ray powder data recorded at room temperature. The refinement was based on the model with all atoms in position $2(e): \pm(x\frac{1}{4}z)$ of space group $P2_1/m$ as reported previously (1).

The intensities of the stronger diffraction lines were measured by planimetering of the diffracto-grams, the intensities of the weaker lines were derived from the peak intensities. Atomic parameters were determined in three different ways: (i) from Fourier syntheses; (ii) by a refinement procedure which searches the set of parameters giving a minimum of $\Sigma w(I_0 - I_c)^2$, as described by Bhuiya and Stanley (5); (iii) by a least-squares procedure. The intensities of all 170 observed diffraction lines were included in procedures (i) and (ii), while only the intensities measured by planimetering were used in the least-squares refinement (iii); the calculations were performed with the TR4 computer of this University.

The atomic parameters given in Table I are averages of the final parameters of procedures (i),

TABLE I

ATOMIC PARAMETERS OF Mo_2S_3

	x	z
Mo(1)	0.310	0.009
Mo(2)	0.108	0.632
S(1)	0.505	0.803
S(2)	0.963	0.161
S(3)	0.729	0.516

(ii), and (iii); from the consistence of the three sets of data the accuracy of the parameters is estimated as 0.001^5 for the metal atoms and 0.005 for sulfur. Interatomic distances are listed in Table II; their accuracy is estimated as 0.04 Å for Mo–S and as 0.02 Å for Mo–Mo. With an overall temperature factor B of 1.27 Å^2 the intensity agreement $\Sigma|I_0 - I_c|/\Sigma I_0$ was 0.25 for all 170 observed lines, which is less satisfactory than is usual for the experimental and refinement procedures applied.

Since needle-shaped crystals—the needle axis coinciding with the b axis—had been obtained in the mean time, it was decided to reinvestigate the structure by single-crystal methods. Weak super-reflections observed in the rotation and Weissenberg photographs taken at room temperature revealed, however, that all axes of the unit cell of $Mo_{2.06}S_3$ should be doubled; the derived structure is a substructure of the true structure at room temperature. Since the intensities of the superreflections in the single-crystal diagrams were too weak to be estimated accurately, no attempt was made to refine the true (super)structure.

In spite of this complication the main features of the structure of $Mo_{2.06}S_3$ are well established (Fig. 2). The structure is based on a close packing of sulfur atoms of the type chh (6). The metal atoms lie in part of the octahedral holes of this packing; they
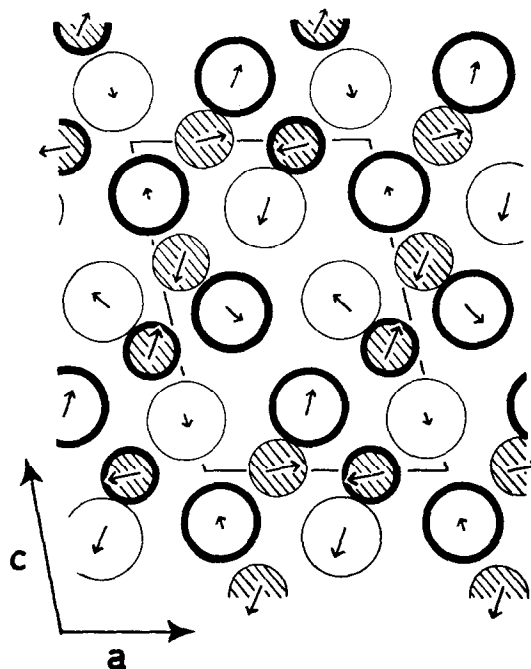

FIG. 2. The (sub)structure of $Mo_{2.06}S_3$ projected along the b axis. Metal atoms are indicated by hatched circles, sulfur by open circles. Atoms at $y = \frac{1}{4}$ are drawn with light contours, atoms at $y = \frac{3}{4}$ with heavy contours. The arrows indicate the displacements of the atoms from positions in an "ideal" lattice (with sulfur in close packing chh and the metal in the centers of octahedral holes) $2\frac{1}{2}$ times enlarged.

are, however, displaced from the octahedron centers in such a way that infinite zigzag Mo–Mo chains are formed running in the b direction. The Mo–Mo distances in these chains are 2.86 Å, which is only slightly longer than the distances of 2.725 Å in bcc molybdenum metal. A more detailed discussion of the structure has been given for the isotypic compounds Nb_2Se_3 and Ta_2Se_3 (7) (where no superreflections were observed).

Phase transitions

As stated, single-crystal diagrams of $Mo_{2.06}S_3$ taken at room temperature contained weak super-reflections indicating that all axes should be doubled. In single-crystal diagrams taken at about 100°C, however, the superreflections were absent. High-temperature Guinier diagrams confirmed that the superlines due to doubling of the b axis disappeared between 20 and 50°C. (The superreflections due to doubling of the a and c axes are too weak to be observable in Guinier diagrams.) Obviously, a phase transition had taken place. Indeed, differential

TABLE II

INTERATOMIC DISTANCES IN Mo_2S_3 (in Å)

Mo(1)–1S(1)	2.34	Mo(2)–1S(3)	2.31
–2S(1)	2.39	–2S(3)	2.40
–2S(2)	2.54	–2S(2)	2.51
–1S(2)	2.72	–1S(1)	2.55
Mo(1)–2Mo(1)	2.85	Mo(2)–2Mo(2)	2.87
–2Mo(1)	3.208	–2Mo(2)	3.208
–1Mo(2)	3.22	–1Mo(1)	3.22

thermal analysis showed a small endothermic effect at $+37°C$ (when heating). No further transitions were found at higher temperatures (up to $800°C$).

However, another phase transition was found by means of a low-temperature Guinier camera. At about $-100°C$ most diffraction lines of $Mo_{2.06}S_3$ split into two components; the compound is triclinic at low temperatures. The unit-cell dimensions at $-150°C$ were found to be:

$$a = 6.06 \text{ Å}; \quad b = 2 \times 3.19 \text{ Å}; \quad c = 8.60 \text{ Å};$$

$$\alpha = 89.6°; \quad \beta = 102.5°; \quad \gamma = 90.3°.$$

By differential thermal analysis the transition was found to be weakly endothermic and to occur at $-80°C$ when heating; the transition shows a pronounced hysteresis.

The transitions of $Mo_{2.06}S_3$ are also reflected in the electrical and magnetic properties (Fig. 3). A detailed discussion of these properties will be given elsewhere (8).

Related Phases

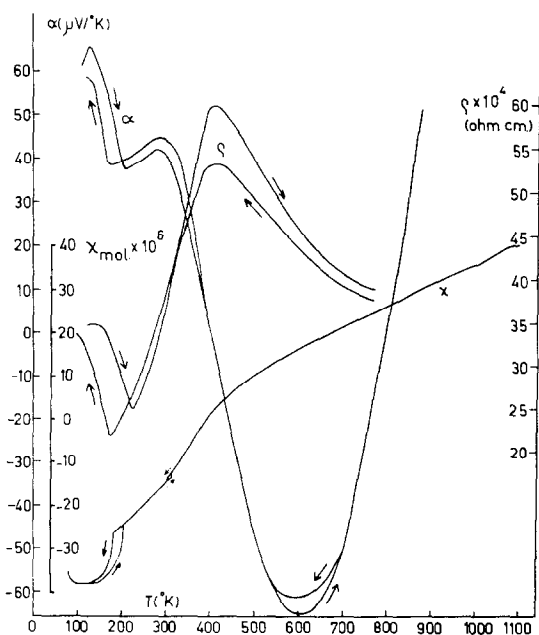While Nb_2Se_3 and Ta_2Se_3 (7) are isotypic with the high-temperature form of $Mo_{2.06}S_3$, Nb_2S_3 has

a quite different structure (9), whereas Mo_2Se_3 does not exist (10, 11). However, a large part of the metal atoms of Nb_2Se_3 can be substituted by molybdenum without change of the structure; for $MoNbSe_3$ we found the following unit-cell dimensions: $a = 6.439 \text{ Å}$; $b = 3.414 \text{ Å}$; $c = 9.111 \text{ Å}$; $\beta = 103.55°$.

Similarly, we could substitute considerable parts of the metal atoms of $Mo_{2.06}S_3$ by Zr, Nb, or Ta, but only traces by Re. The solid solutions $(Mo_{1-x}, Nb_x)_{2.06}S_3$ (prepared at $1250°C$) were homogeneous for $0 \leqslant x \leqslant 0.5$; the unit-cell dimensions of $Mo_{1.03}Nb_{1.03}S_3$ at room temperature were found as: $a = 6.125 \text{ Å}$; $b = 3.292 \text{ Å}$; $c = 8.692 \text{ Å}$; $\beta = 102.67°$. No indications for a superstructure were found in Guinier diagrams of the solid solutions with $x > 0.025$; the samples remained monoclinic down to $110°K$. The physical properties of $(Mo_{1-x}, Nb_x)_{2.06}S_3$ did not indicate any transition in the range $10-1000°K$, if $x > 0.025$ (8).

In agreement with other investigators (10–12) we found the compounds previously regarded as Mo_2Se_3 and Mo_2Te_3 to have broad ranges of homogeneity which include the composition Mo_3X_4, but not Mo_2X_3. The compounds are monoclinic with $a = 4.632 \text{ Å}$; $b = 4.762 \text{ Å}$; $c = 6.649 \text{ Å}$; $\beta = 92.56°$ for Mo_3Se_4, and $a = 4.875 \text{ Å}$; $b = 5.092 \text{ Å}$; $c = 7.051 \text{ Å}$; $\beta = 93.75°$ for Mo_3Te_4; similar results were recently reported by Bakakin et al. (13). The unit-cell volumes (146.6 Å^3 for the selenide, 170.7 Å^3 for the telluride) are better compatible with an ideal composition of Mo_3X_4 than with Mo_2X_3 (cf. cell volume Nb_3Se_4:$2 \times 150.6 \text{ Å}^3$; Nb_3Te_4:$2 \times 179.8 \text{Å}^3$; Nb_2Se_3:200.2Å^3; $MoNbSe_3$: 194.7 Å^3). No indications for transitions in Mo_3Se_4 or Mo_3Te_4 were found.

FIG. 3. The magnetic susceptibility χ_{mol}, electrical resistivity ρ, and Seebeck coefficient α of $Mo_{2.06}S_3$ as functions of the temperature. The effects of the phase transitions at 194 and $310°K$ (when heating) are clearly seen: the low-temperature transition shows a pronounced hysteresis.

References

1. F. Jellinek, Nature 192, 1065 (1961).
2. C. L. McCabe, J. Metals 7, 61 (1955).
3. N. Morimoto and G. Kullerud, Carnegie Inst. Washington Year Book, Vol. 61, p. 143, 1962.
4. H. U. Lenné, Z. Kristallogr. 116, 190 (1961).
5. A. K. Bhuiya and E. Stanley, Acta Crystallogr. 16, 981 (1963).

6. A. F. WELLS, "Structural Inorganic Chemistry," 3rd ed., p. 114, Clarendon Press, Oxford, 1962.

7. F. KADIJK, R. HUISMAN, AND F. JELLINEK, *Acta Crystallogr. B* **24**, 1102 (1968).

8. R. DE JONGE, Dissertation, Groningen, 1970; R. DE JONGE AND C. HAAS, to be published.

9. F. JELLINEK, G. BRAUER, AND H. MÜLLER, *Nature* **185**, 376 (1960); F. KADIJK AND F. JELLINEK, *J. Less-Common Metals* **19**, 421 (1969).

10. A. A. OPALOVSKII AND V. E. FEDOROV, *Izv. Akad. Nauk SSSR Neorg. Mater.* **2**, 443 (1966).

11. M. SPIESSER, C. MARCHAL, AND J. ROUXEL, *C. R. H. Acad. Sci. Ser. C* **266**, 1583 (1968).

12. M. SPIESSER AND J. ROUXEL, *C. R. H. Acad. Sci. Ser. C* **265**, 92 (1967).

13. V. V. BAKAKIN, YU. I. MIRONOV, A. A. OPALOVSKII, AND V. E. FEDOROV, *Izv. Sib. Otd. Akad. Nauk SSSR, Ser. Khim. Nauk* **3**, 98 (1968).